Continuum kinetic simulations of tokamak edge plasmas with COGENT

Lee Ricketson, Milo Dorr, Mikhail Dorf, Debojyoti Ghosh

Lawrence Livermore National Laboratory

Presented at PASC 2022, June 29, 2022

LLNL-PRES-728137

This work was performed under the auspices of the U.S. Department of Energy by Lawrence Livermore National Laboratory under Contract DE-AC52-07NA27344.

This project is part of the Edge Simulation Laboratory collaboration between US DOE ASCR and FES

Edge Simulation Laboratory

Math (ASCR)

CASC
Center for Applied Scientific Computing

L. Ricketson
M. Dorr
D. Ghosh
P. Tranquilli

BERKELEY LAB

D. Martin
P. Colella
P. Schwartz

Physics (FES)

Fusion Energy Sciences

M. Dorf
V. Geyko
J. Angus

GENERAL ATOMICS AND AFFILIATED COMPANIES

P. Snyder
J. Candy
E. Belli

UC San Diego

S. Krasheninnikov

Cross separatrix transport (Dorf et al., Contrib. Plasma Phys.,58, 434-444 (2018))

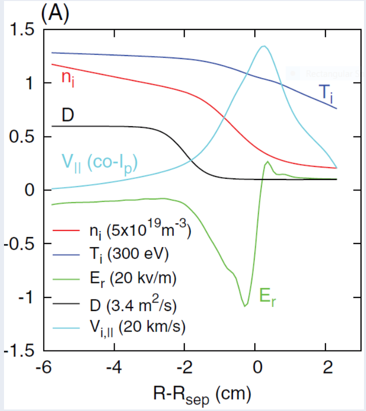

ELM heat pulse (Joseph et al., Nucl. Mater. Energy, 19, 330-334 (2019))

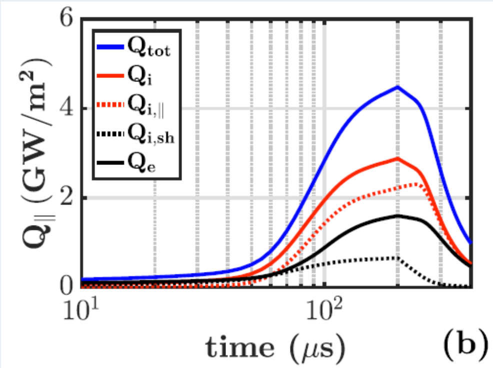

Kinetic drift-wave instability (Lee et al., Contrib. Plasma Phys., 58, 445-450 (2018))

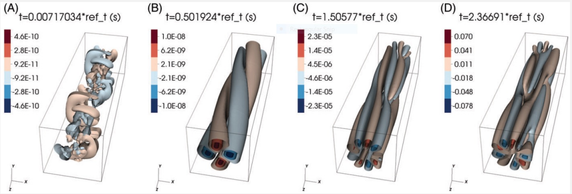

High-order drift wave modeling (Dorf et al., J. Comput. Phys., 373, 446-545 (2018))

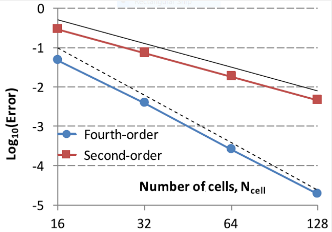

5-D full-f gyrokinetic code COGENT (Dorf et al., Contrib. Plasma Phys. (2020))

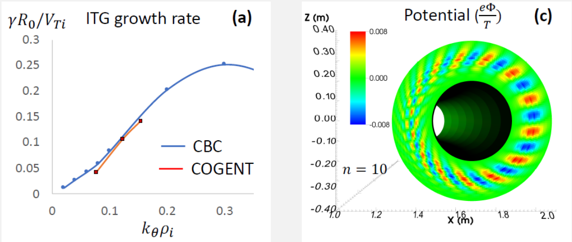

Tokamak edge plasma is challenging to model numerically

- **Kinetic effects are essential**
  - Strong deviations from Maxwellian distribution
  - Large poloidal variations in electrostatic potential
  - Fully nonlinear collision operator
- **More complicated geometry**
  - Magnetic separatrix
  - Boundaries
- **Collision regimes vary rapidly**
  - Hot core region – weakly collisional
  - Cold outer region – strongly collisional

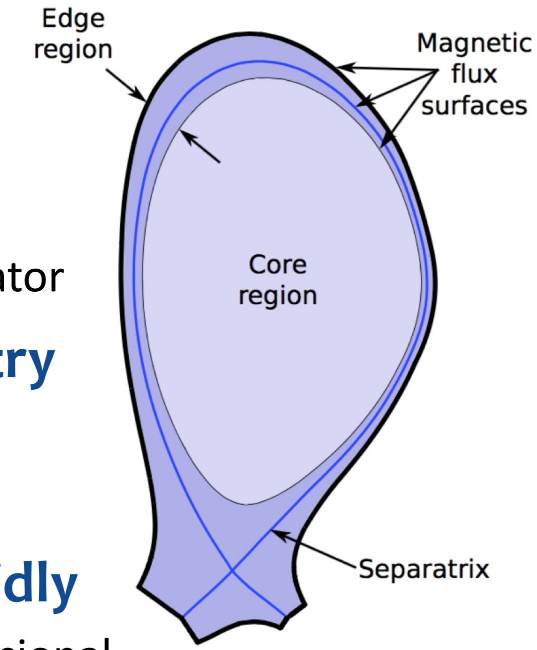

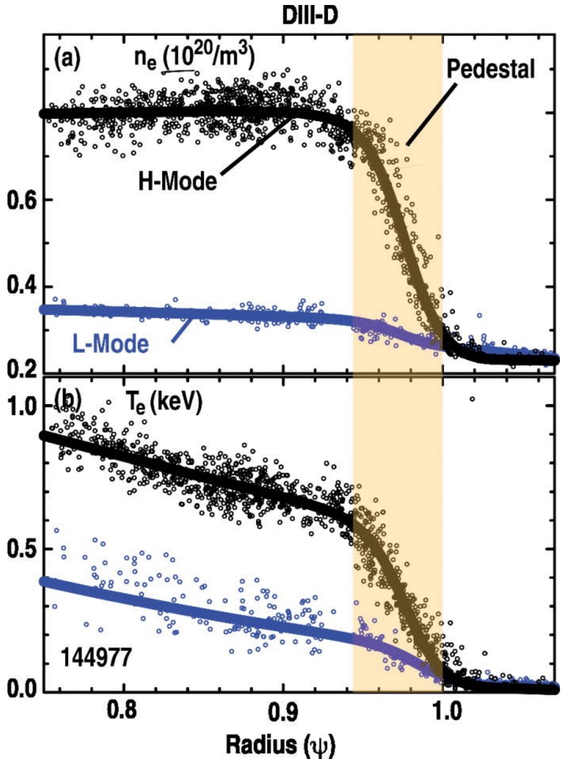

[A. W. Leonard, Phys. Plasmas 21, 090501 (2014)]

Dynamics in the edge region are characterized by a large range of scales

Tokamaks and Gyrokinetics

- Tokamak = toroidal magnetic confinement fusion device
- Strong non-equilibrium behavior requires kinetic modeling

$$\frac{\partial(B_\parallel^* f)}{\partial_t} + \nabla_{\mathbf{R}} \cdot \left(\dot{\mathbf{R}}[f]f\right) + \frac{\partial}{\partial v_\parallel}\left(\dot{v}_\parallel[f]f\right) = \mathcal{C}[f]$$

$$\text{Unknown:} \quad f(\mathbf{R}, v_\parallel, \mu), \qquad \mathbf{R} \in \mathbb{R}^3$$

- Strong magnetic field →
  - Asymptotic limit… 6D to 5D
  - Anisotropy
- Numerical challenges include:
  - Complex geometry
  - High dimensionality
  - Conservation
  - Positivity
  - Multiple space and ***time scales***

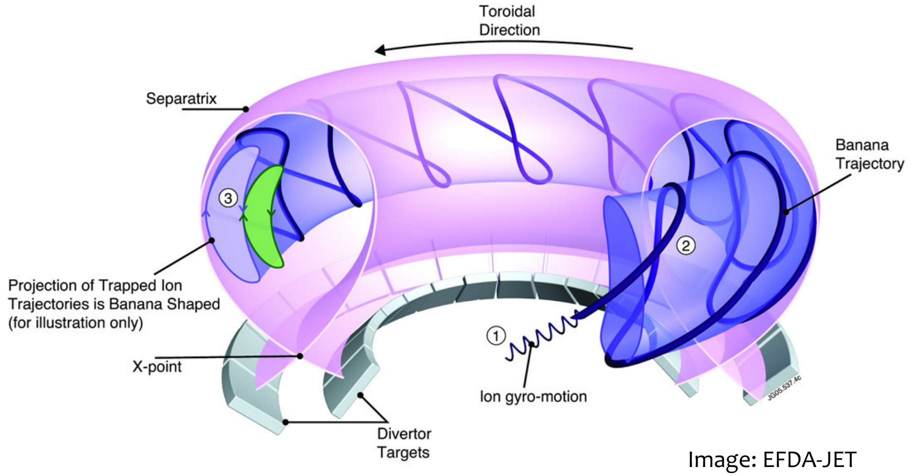

Image: EFDA-JET

$$\dot{\mathbf{R}} \equiv v_\parallel \mathbf{B}^* + \frac{\rho_L}{Z}\mathbf{b} \times \mathbf{G} \qquad \mathbf{G} \equiv Z\nabla_{\mathbf{R}}\Phi + \frac{\mu}{2}\nabla_{\mathbf{R}}B$$

$$\dot{v}_\parallel \equiv -\frac{1}{m}\mathbf{B}^* \cdot \mathbf{G} \qquad \mathbf{B}^* \equiv \mathbf{B} + \rho_L \frac{m v_\parallel}{Z}\nabla_{\mathbf{R}} \times \mathbf{b}$$

- Advection couples to self-consistent field
- Parallel advection >> perpendicular drifts
  - Leads to strong anisotropy

Design decisions motivated by numerical challenges

▪ High Dimensionality	motivates	High-order Later, w/ sparse grids
▪ Conservation	motivates	Finite Volume
▪ Anisotropy	motivates	Mapped, field-aligned grids
▪ Complex Geometry	motivates	Multiblock meshing
▪ Multiple Scales	motivates	IMEX time integration

High-order, mapped finite volume discretization

Computational coordinates:

Spatial domain discretized by rectangular control volumes

$$V_{\mathbf{i}} = \prod_{d=1}^{D}\left[i_d - \frac{h}{2}, i_d + \frac{h}{2}\right]$$

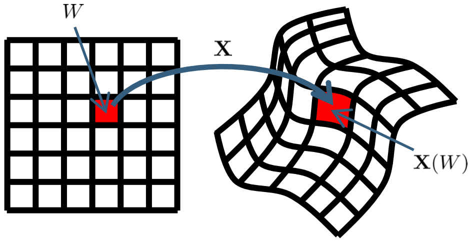

$\mathbf{X} \equiv \mathbf{X}(\xi), \quad \mathbf{X} : [0,1]^D \rightarrow \Omega \subset \mathbf{R}^D$

Mapped coordinates:

Mapping from abstract Cartesian coordinates into physical space

$$\mathbf{X} = \mathbf{X}(\boldsymbol{\xi}), \qquad \mathbf{X} : [0,1]^D \longrightarrow \mathbb{R}^D$$

Fourth-order flux divergence average from fourth-order cell face averages

$$\int_{\mathbf{X}(V_{\mathbf{i}})} \nabla_{\mathbf{X}}\cdot\mathbf{F}d\mathbf{x} = \sum_{\pm=+,-}\sum_{d=1}^{D}\pm\int_{A_d^{\pm}}\left(\mathbf{N}^T\mathbf{F}\right)_d d\mathbf{A}_{\boldsymbol{\xi}} = h^{D-1}\sum_{\pm=+,-}\sum_{d=1}^{D}\pm F^d_{\mathbf{i}\pm\frac{1}{2}\mathbf{e}^d} + O\left(h^4\right)$$

where

$$\left(\mathbf{N}^T\right)_{p,q} = \det\left(\mathbf{R}_p\left(\frac{\partial\mathbf{X}}{\partial\boldsymbol{\xi}}, \mathbf{e}^q\right)\right)$$

$\mathbf{R}_p\left(\mathbf{A}, \mathbf{v}\right)$**: replace *p*-th row of** $\mathbf{A}$ **with** $\mathbf{v}$

$$F^d_{\mathbf{i}\pm\frac{1}{2}\mathbf{e}^d} = \sum_{s=1}^{D}\langle N^s_d\rangle_{\mathbf{i}\pm\frac{1}{2}\mathbf{e}^d}\langle F^s\rangle_{\mathbf{i}\pm\frac{1}{2}\mathbf{e}^d} + \frac{h^2}{12}\sum_{s=1}^{D}\left(\mathbf{G}_0^{\perp,d}\left(\langle N^s_d\rangle_{\mathbf{i}\pm\frac{1}{2}\mathbf{e}^d}\right)\right)\cdot\left(\mathbf{G}_0^{\perp,d}\left(\langle F^s\rangle_{\mathbf{i}\pm\frac{1}{2}\mathbf{e}^d}\right)\right)$$

$\mathbf{G}_0^{\perp,d} =$ **second-order accurate centered difference of** $\nabla_{\boldsymbol{\xi}} - \mathbf{e}^d\dfrac{\partial}{\partial\xi_d}$

$$\langle q\rangle_{\mathbf{i}\pm\frac{1}{2}\mathbf{e}^d} \equiv \frac{1}{h^{D-1}}\int_{A_d} q(\boldsymbol{\xi})d\mathbf{A}_{\boldsymbol{\xi}} + O\left(h^4\right)$$

We use multiblock grid technology to discretize the edge domain

- **Separatrix partitions edge into three regions:**
  - Core, Private flux, Scrape-off
- **Regions mapped to disjoint union of uniformly-gridded rectangular blocks**
  - Each block decomposed into boxes
- **High-order MMB finite-volume formalism requires extended smooth block mappings***
- **One coordinate of mapping parameterizes flux surfaces**
- **Flux-surface alignment abandoned near the X-point to avoid singular metrics****

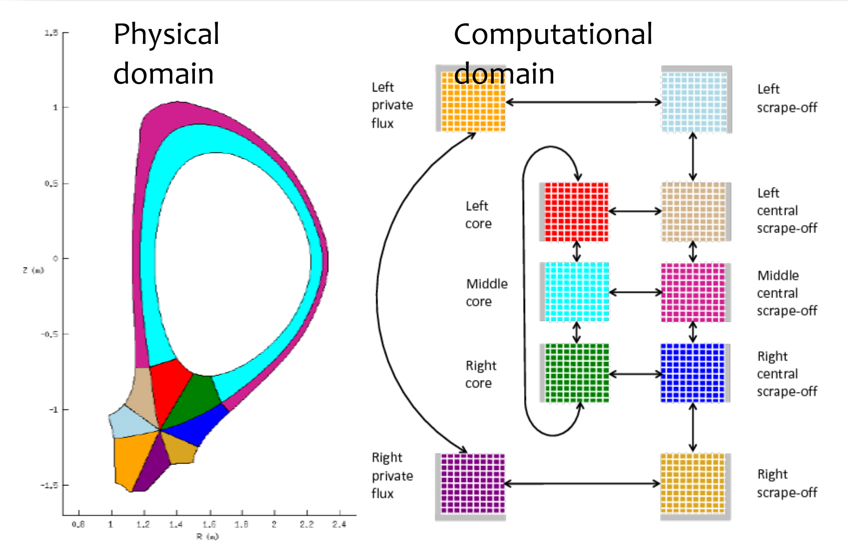

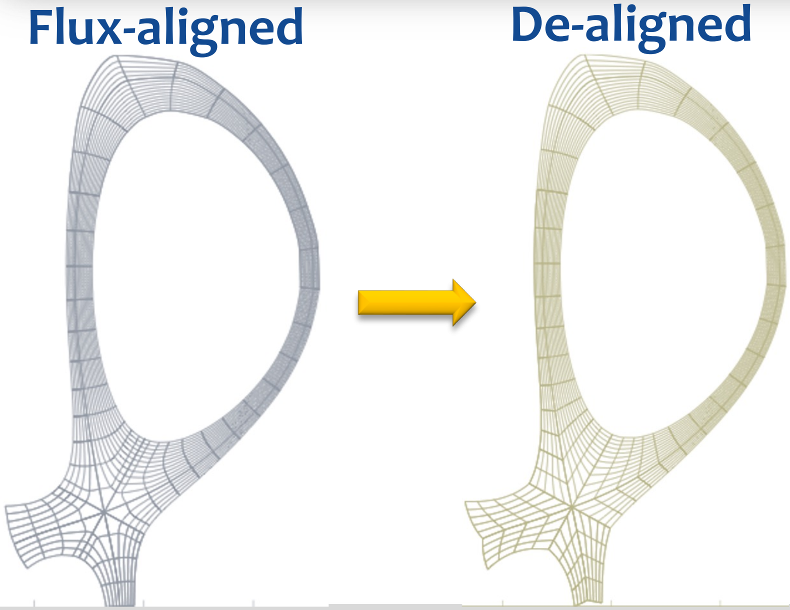

*[McCorquodale. et al. (2015) *J. Comput. Phys.* **288** 181-195]

[Dorr. Et al. (2018) *J. Comput. Phys.* **373 605-630]

Extended COGENT to 5-D, field aligned coordinates in realistic geometries

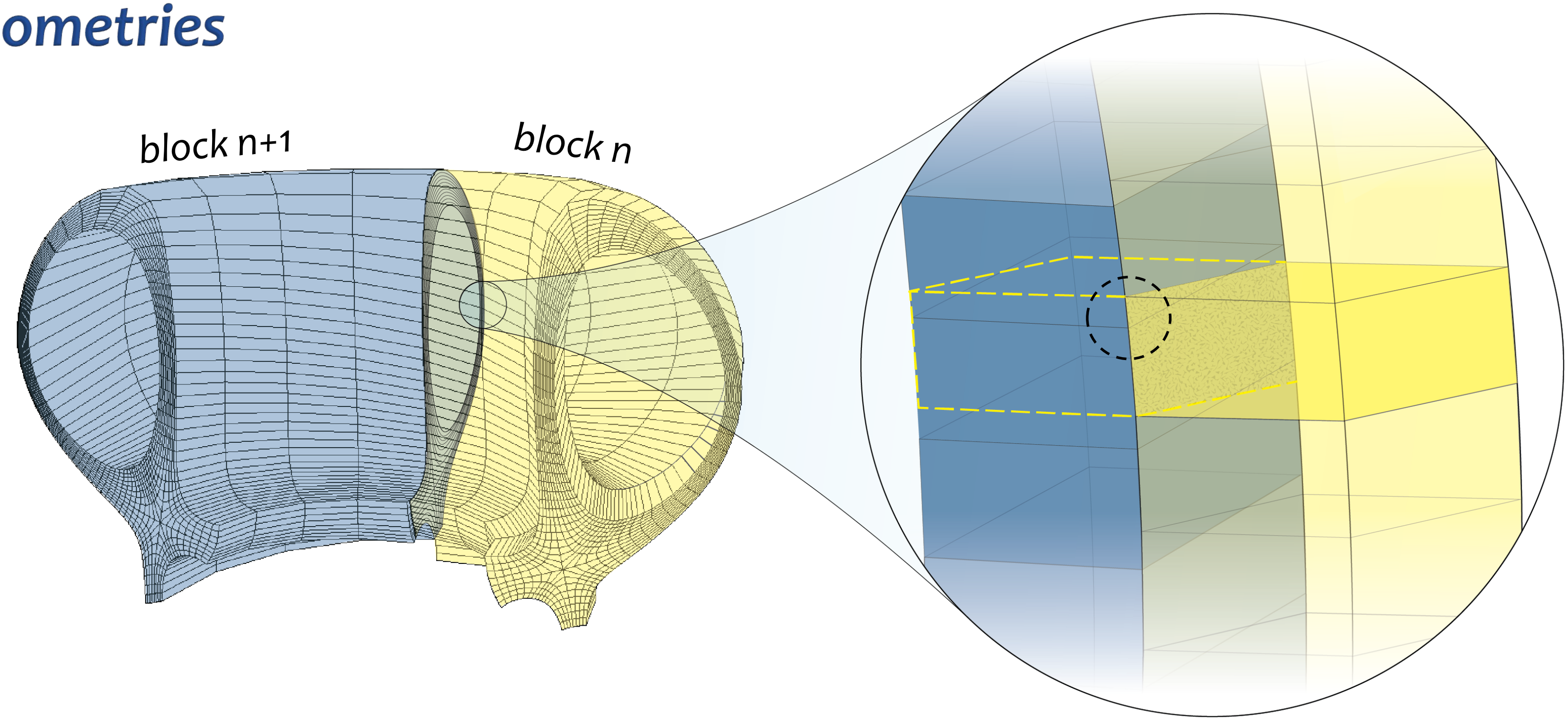

- Existing technology assumed conformality of mesh faces at block boundaries
- Radially varying shears make this conformality impossible
- Approach has been extended to allow non-conformality in *one dimension*
- Current implementation is 2nd-order, non-conservative
- High-order, conservative formulation in progress

Multiple time-scales arising from multiple physical phenomena

$$\frac{\partial f_i}{\partial t} + \nabla_\parallel \cdot \left(\dot{\mathbf{R}} f_i\right) + \nabla_\perp \cdot \left(\dot{\mathbf{R}} f_i\right) + \partial_{v_\parallel}(\dot{v}_\parallel f_i) = C_i(f_i) + \nabla_\perp \cdot (D_{AN} \nabla_\perp f_i)$$

$$\frac{\partial f_e}{\partial t} + \nabla_\parallel \cdot \left(\dot{\mathbf{R}} f_e\right) + \nabla_\perp \cdot \left(\dot{\mathbf{R}} f_e\right) + \partial_{v_\parallel}(\dot{v}_\parallel f_e) = C_e(f_e) + \nabla_\perp \cdot (D_{AN} \nabla_\perp f_e)$$

Faster

↕

Slower

Time scale	ω
Electrostatic Alfven waves	$(V_{Te}/qR)\,(L/\rho_s)$
Electron parallel streaming & collisions	$V_{Te}/qR\,, \nu_e$
Ion parallel streaming & collisions	$V_{Ti}/qR\,, \nu_i$
Drift ion-scale turbulence	V_s/L
Transport (profile evolution)	$D_{AN}/L^2,\ \nu_i \rho_i^2/L^2$

<u>General Preconditioning Strategies</u>:

- Exploit physics-based closure models
- Lower-order discretizations

IMEX methods to address multiple scales

Spatial discretization yields semi-discrete ODE in time

$$\frac{d\tilde{f}}{dt} = \mathcal{R}\left(\tilde{f}\right) \equiv \underbrace{\mathcal{V}\left(\tilde{f}\right)} + \underbrace{\mathcal{C}\left(\tilde{f}\right)}$$

Spatially-discretized **Vlasov** and **collisions** terms

Explicit time integration:
Runge-Kutta methods

$$\Delta t\left(\lambda\left[\frac{d\mathcal{R}\left(\tilde{f}\right)}{d\tilde{f}}\right]\right) \in \{z : |R(z)| \le 1\}$$

Time step constrained by eigenvalues (time scales) of *entire RHS*

Implicit-Explicit (IMEX) time integration:
Additive Runge-Kutta (ARK) methods

$$\mathcal{R}\left(\tilde{f}\right) = \underbrace{\mathcal{R}_{\text{stiff}}\left(\tilde{f}\right)}_{\text{Implicit}} + \underbrace{\mathcal{R}_{\text{nonstiff}}\left(\tilde{f}\right)}_{\text{Explicit}}$$

$$\Delta t\left(\lambda\left[\frac{d\mathcal{R}_{\text{nonstiff}}\left(\tilde{f}\right)}{d\tilde{f}}\right]\right) \in \{z : |R(z)| \le 1\}$$

Specifically: Additive Runge Kutta (ARK) Methods

Diagonal implicitness

Stage Solves:

$$\tilde{f}^{(i)} = \tilde{f}_n + \Delta t \left\{ \sum_{j=1}^{i-1} a_{ij} \mathcal{R}_{\text{nonstiff}} \left(\tilde{f}^{(j)} \right) + \sum_{j=1}^{i} \tilde{a}_{ij} \mathcal{R}_{\text{stiff}} \left(\tilde{f}^{(j)} \right) \right\}$$

Step Completion:

$$\tilde{f}_{n+1} = \tilde{f}_n + \Delta t \sum_{i=1}^{s} b_i \left\{ \mathcal{R}_{\text{nonstiff}} \left(\tilde{f}^{(j)} \right) + \mathcal{R}_{\text{stiff}} \left(\tilde{f}^{(j)} \right) \right\}$$

Stage solves done with Jacobian-Free Newton Krylov

Matrix to be inverted at each Newton iteration of the form

$$\left(\mathcal{I} - \Delta t \frac{d\mathcal{R}_{\text{stiff}}}{d\tilde{f}} \right)$$

Flexible preconditioning framework

<u>Expectation</u>: Different physics problems feature different terms requiring implicitness

<u>Needed</u>: Flexible handling of arbitrary # of implicit terms

<u>Developed</u>: Multiphysics operator-split preconditioning framework

$$I + \Delta t \sum_k A_k \approx \prod_k (I + \Delta t A_k)$$

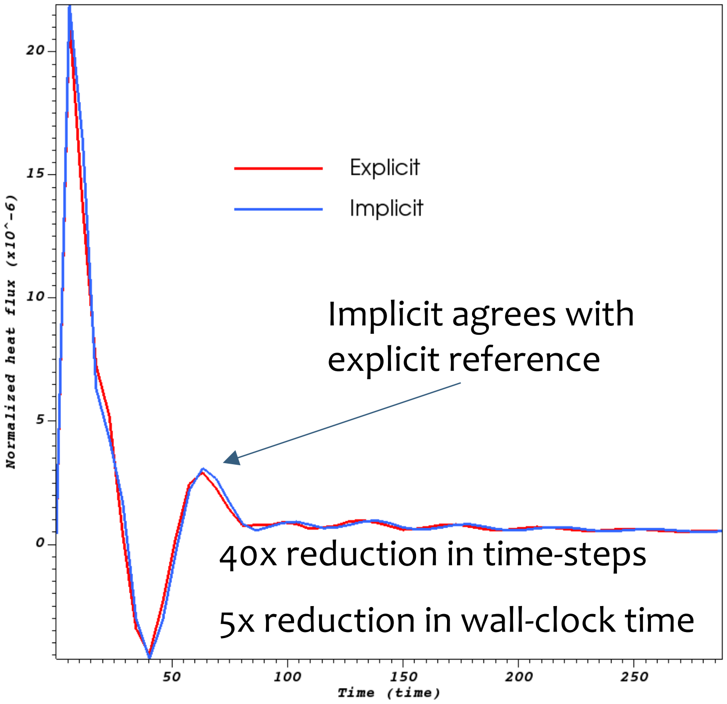

Implicit agrees with explicit reference

40x reduction in time-steps

5x reduction in wall-clock time

Independent preconditioning allows physics-based approaches for individual terms:

Allows better efficiency than a monolithic strategy ever could, but **<u>still need to design individual preconditioners</u>**

Case Study: Electron Vorticity Model

- Electron dynamics typically faster than ions by factor of $\sqrt{m_i/m_e} \approx 60$ which motivates
  - Implicit treatment of electrons, and/or…
  - Reduced models of electron behavior
- Usual adiabatic approximation no good for edge physics, so made our own reduced model for electrostatic potential:

$$\frac{\partial \omega}{\partial t} + \nabla \cdot (\mathbf{V}[f]\omega) - \nabla_{\|} \left[\frac{\sigma}{e} \left(\frac{1}{n_i} \nabla_{\|} (n_e T_e) - e \nabla_{\|} \phi \right) \right] = g[f] \qquad \sigma \gg 1$$

$$\omega = -M\phi \qquad\qquad n_e = n_i + e^{-1}\omega$$

2nd order elliptic operator

Small (but physically important) <u>polarization correction</u>… makes system 4th order

Without Polarization Correction

- "Freeze" coefficients at previous Newton iterate to make preconditioning system linear
- Stage preconditioning solve becomes

$$\left(\alpha M - \Delta t \nabla_{\|} \sigma \nabla_{\|}\right) \phi = r$$

- Highly anisotropic 2nd order elliptic operator
- Solve with *hypre* AMG solver
  - Well-suited to automatically dealing with anisotropy

Physical Importance of Polarization Correction

- In simplified problem, linear growth rate maximized when

$$\frac{k_\parallel^2}{k_\perp^3}\frac{\omega_{ci}\omega_{ce}^2}{0.51\nu_e}\frac{L_n}{V_{Te}^2}\left(1+k_\perp^2\rho_s^2\right)\approx 1$$

Due to polarization correction

Without correction, unstable modes may have arbitrarily short wavelength

Grid-scale instabilities in code

With Polarization Correction

- Preconditioner stage system becomes

$$\left[\alpha M - \Delta t\left(\nabla_{\|}\sigma\nabla_{\|} + \underbrace{\nabla_{\|}\frac{\sigma}{en_i}\nabla_{\|}T_e M}_{\text{4th-order piece}}\right)\right]\phi = r$$

- Want to avoid direct implementation of 4th order term b/c 4th order stencils across block boundaries introduce high complexity in multiblock geometry

- Instead, introduce auxiliary variable:

$$\begin{pmatrix} \alpha M - \Delta t\nabla_{\|}\sigma\nabla_{\|} & \nabla_{\|}\frac{\sigma}{en_i}\nabla_{\|}T_e \\ M & I \end{pmatrix}\begin{pmatrix} \phi \\ \omega_{aux} \end{pmatrix} = \begin{pmatrix} r \\ 0 \end{pmatrix}$$

- Schur Complement

$$I - M\left(\alpha M - \Delta t\nabla_{\|}\sigma\nabla_{\|}\right)^{-1}\nabla_{\|}\frac{\sigma}{en_i}\nabla_{\|}T_e$$

is well-conditioned and already have solver for part we need to invert

- Solved with *hypre* MGR

Enabling novel physics results

- Combination of many technologies enables first-of-kind physics studies
- First continuum, cross-separatrix simulation of ion-scale tokamak turbulence

Many physics effects still to be added… opportunities for optimization

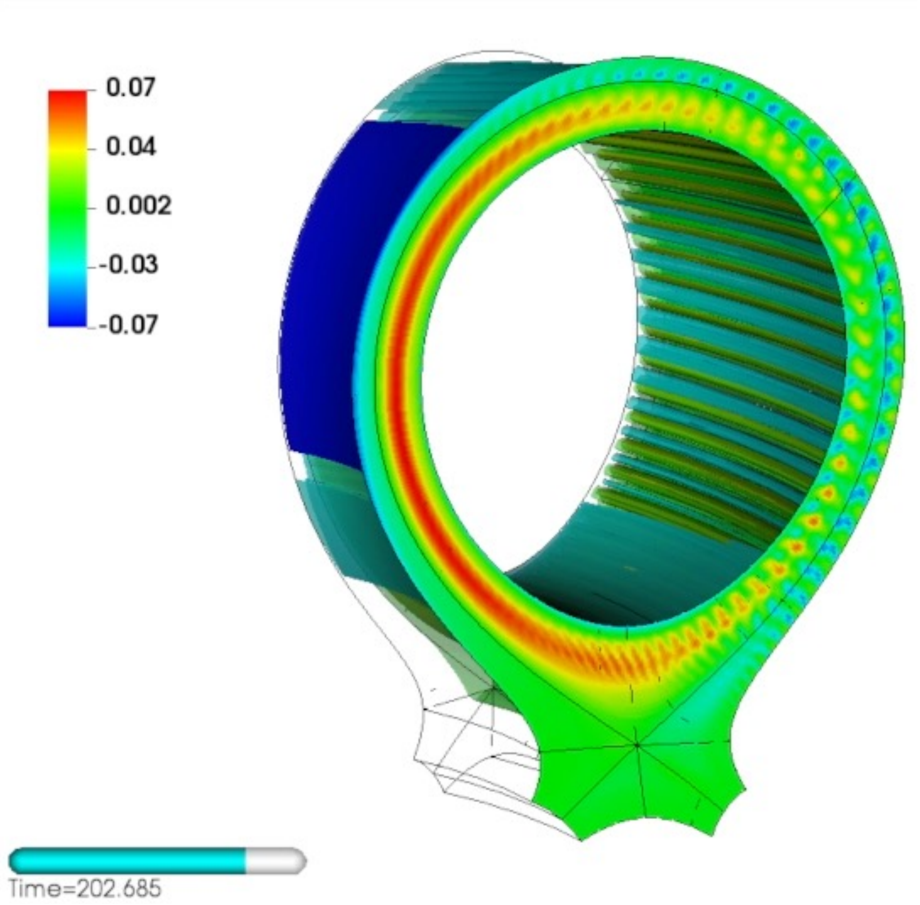

Advection

- Another approach to dealing with electron time-scales:
  - Step over their fast advection by treating their kinetic equation implicitly
  - CFL restrictions of fine mesh make implicit advection even more attractive

- Current solver/preconditioning approach: “Freeze” nonlinearity in advection coefficients

$$\left[\alpha I + \Delta t \left(\nabla_x \cdot \dot{\mathbf{R}}\left[f^{n}\right] + \nabla_v \cdot \dot{v}_{||}\left[f^{n}\right]\right)\right] \delta f^{n+1} = r$$

Time-step

Implicit electron advection in ELM studies

- Edge-localized modes (ELMs) are a disruptive instability that can damage wall materials if uncontrolled
- Requires kinetic electrons – vorticity model insufficient – to capture
- Implicit electron treatment enables time-step closer to ion time-scales
- No artificial modification of electron mass
- Still limited by electrostatic Alfvén wave frequency……

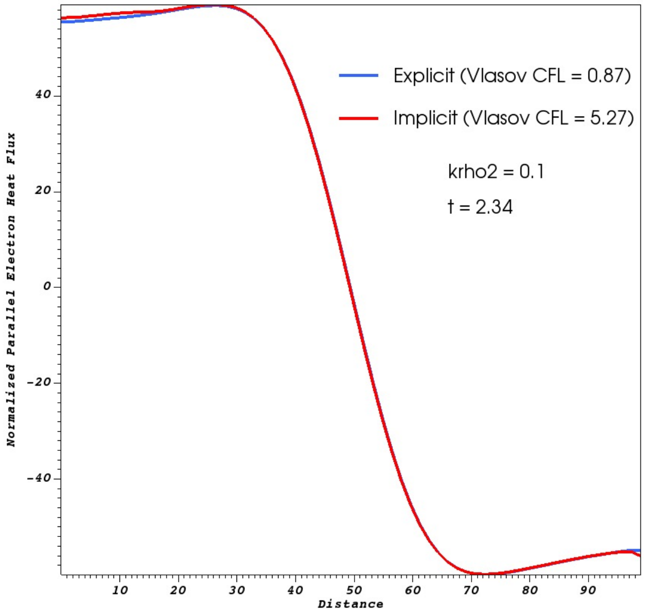

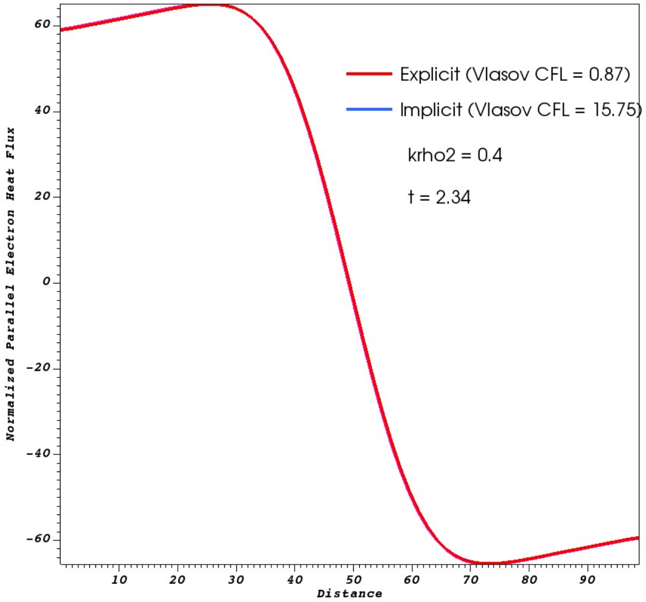

Work performed as part of the DOE FES/ASCR Plasma Surface Interactions 2 SciDAC project https://collab.cels.anl.gov/display/PSIscidac2

Open Problem – Electrostatic Alfvén Wave (ESAW)

- Coupling to electric field results in wave with frequency

$$\omega = \omega_{ci}\sqrt{\frac{m_i}{m_e}}\frac{k_\parallel}{k_\perp}$$

Fast cyclotron frequency

- Very fast but physically unimportant
- Stepping over requires implicit treatment of parallel fields
- So, need Jacobian of $\dot{v}_\parallel[f] \propto \nabla_\parallel \phi$ but

$$M\phi = \int f dv_\parallel d\mu \implies \text{“semi-dense” Jacobian}$$

- Idea: Use fluid model to approximate Jacobian… work in progress

We began exploring the utility of sparse grids in COGENT

For a pth-order discretization on a mesh with cell size *h* in *d* dimensions

$\kappa \propto h^{-d}$	$\epsilon \propto h^p$	$\Longrightarrow$	$\kappa \propto \epsilon^{-d/p}$
Complexity	Error		Efficiency

Combination technique: Assume an error relation of the form

$$f - \widetilde{f} = C_1(h_x)h_x^p + C_2(h_y)h_y^p + C_3(h_x,h_y)h_x^p h_y^p$$

with C_i bounded. Letting

$$f_n = \sum_{i+j=n+1} f_{i,j} - \sum_{i+j=n} f_{i,j}$$

then

$$\kappa \propto h^{-1}|\log(h)|^{d-1} \qquad \epsilon \propto h^p|\log(h)|^{d-1}$$

$$\Longrightarrow \qquad \kappa \propto \epsilon^{-1/p}|\log(\epsilon)|^{(d-1)(1+1/p)}$$

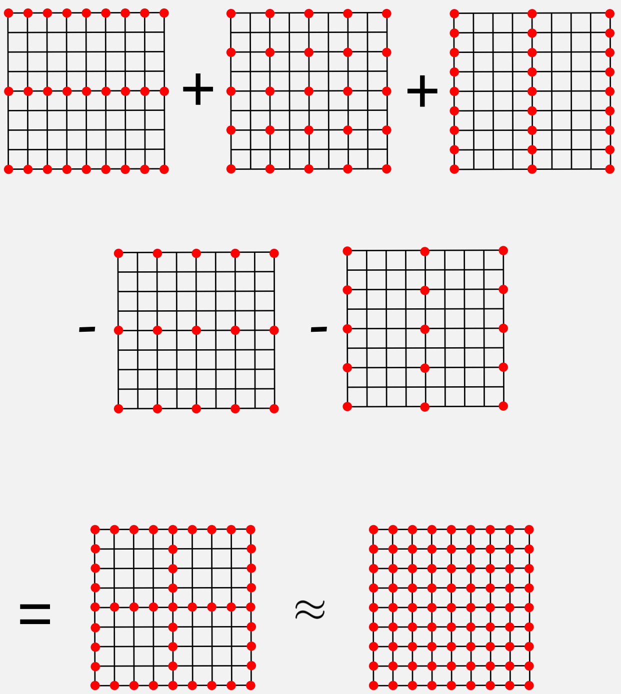

Sparse grid methods have been investigated for high-dimensional kinetic simulations

L. F. Ricketson and A. J. Cerfon, Plasma Phys. Contr. F. 59, 2 (2016)

W. Guo and Y. Cheng, SISC (2016)… and others

We developed a new sparse-grid, high-order finite volume method

- Standard stencils for high-order FV schemes are incompatible with sparse grids
- Developed new stencils that satisfy the constraints on error expansion
- Implementation in COGENT ongoing

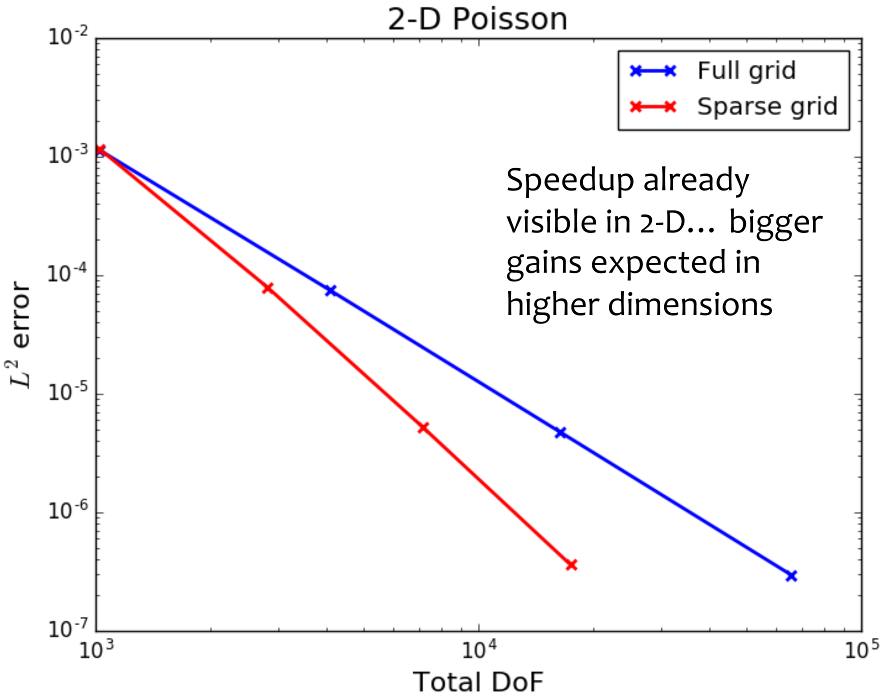

Speedup already visible in 2-D… bigger gains expected in higher dimensions

Sample solution in tokamak geometry

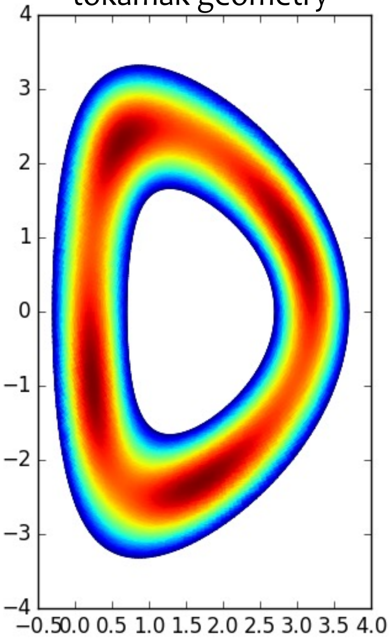

Old Stencil

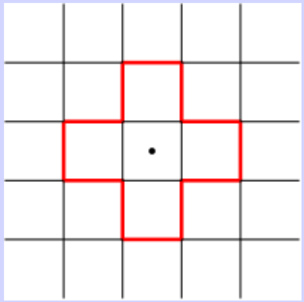

$$\varepsilon = C_1 h_x^4 + C_2 h_y^4 + C_3 h_x^2 h_y^2$$

New Stencil

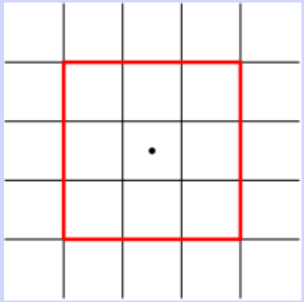

$$\varepsilon = C_1 h_x^4 + C_2 h_y^4 + C_3 h_x^4 h_y^4$$

Sparse Grid implementation in COGENT

- Framework for combining solutions on multiple grids implemented
- Tested on simple problems with ”old” stencils
    - Linear advection
    - Drift wave instability
- Confirm 2nd order convergence
- Implementation of new stencils for 4th order convergence in progress, but buggy…

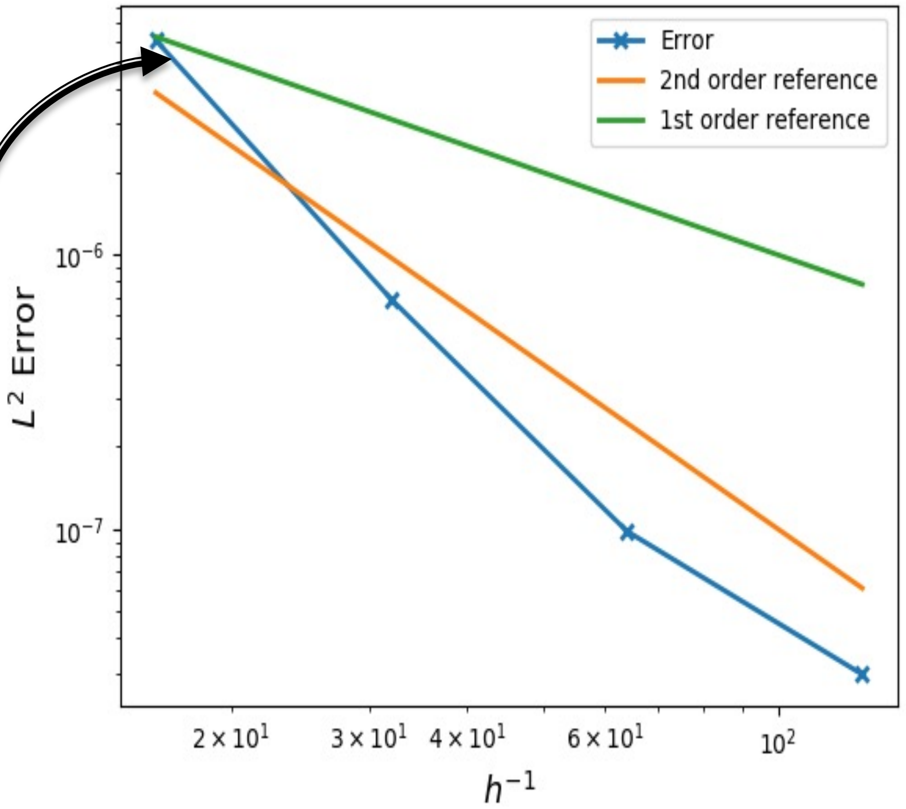

Conclusions

- COGENT = High-order mapped multblock code for tokamak edge with <u>flexible IMEX time integration framework</u>
- Multiple stiff physical scales provide unique preconditioning challenges… need tailored approaches for each
- Work ongoing, but
  - Block-preconditioning of 4th-order vorticity model shows promising results
  - Implicit advection already aiding physics studies, with additional ESAW challenges to be tackled

CASC

Center for Applied
Scientific Computing

Lawrence Livermore
National Laboratory